Proceedings of 20th International Congress on Acoustics, ICA 2010

23-27 August 2010, Sydney, Australia

Numerical investigation of ultrasound wave propagation in cancellous bone with oblique trabecular orientation

Atsushi Hosokawa

Akashi National College of Technology, Akashi, Japan

PACS: 43.80.Cs, 43.20.Bi

ABSTRACT

Two longitudinal waves of "fast and slow waves" propagating through cancellous bone can be separately observed in the case of the trabecular structure oriented parallel to the wave propagation, but a single wave, in which the fast and slow waves completely overlap, can be observed in the case of the perpendicularly oriented structure. This can be considered to be because the propagation paths of the fast and slow waves in these cases are different. In this study, the changes in the propagation paths (or directions) with the angle of the trabecular orientation have been numerically investigated using finite-difference time-domain simulations with realistic cancellous bone models reconstructed from a three-dimensional microcomputed tomographic image. The simulated results suggested that both propagation paths changed owing to the oblique trabecular orientation, which could affect the structural dependences of the propagation properties.

INTRODUCTION

To reduce fracture risks, early detection and treatment for osteoporosis are important. Ultrasound techniques are very useful for early detection because of high advantages of safety and convenience. However, ultrasound techniques are less accurate than X-ray techniques typified by dual energy X-ray absorptiometry (DXA). This is because the propagation phenomena of ultrasound waves in bone, particularly in cancellous bone, are not yet sufficiently elucidated. Cancellous bone has a complex trabecular structure, which can largely affect the ultrasound propagation in the bone [1-6]. It was demonstrated that two longitudinal waves of "fast and slow waves" could be separately observed for the trabecular structure oriented in the propagation direction [1], but that only a single wave was observed for the trabecular orientation perpendicular to the propagation [3]. Among the commonly used ultrasound technique, the speed of sound (SOS) and broadband ultrasound attenuation (BUA) of the single wave are measured at the site including cancellous bone with a perpendicular trabecular orientation [7-12] On the other hand, a novel technique for osteoporosis considering the propagation of the fast and slow waves in a trabecular-oriented direction has been recently developed [13-16].

The ultrasound propagation in each case of the parallel and perpendicular trabecular orientations has been investigated in many studies [4-6, 17-21], but the propagation in the case of the oblique orientation has not sufficiently been clarified. It can be expected that the oblique trabecular orientation may affect the ultrasound propagation, e.g., the propagation path (or direction) may change with the oriented angle. In a previous study [22] using stratified cancellous bone phantoms composed of periodically alternating solid (trabecular) and fluid (water) layers, in fact, it was shown that the fast and slow waves tended to propagate along the orientation of the trabecular layers. In this study, the propagation paths of the fast and slow waves in cancellous bone with oblique trabecular orientation were simulated using a finite-difference time-domain (FDTD) method, and it was investigated which each wave could propagate along the orientation, across the orientation, or straight without relation to the orientation. Then, numerical models of cancellous bone were reconstructed from a three-dimensional (3D) microcomputed tomographic (μCT) image.

SIMULATION METHOD

Cancellous bone model

Figure 1 shows the schematic of the simulation model for observing the ultrasound propagation through cancellous bone with oblique trabecular orientation. A cancellous bone specimen of approximately 10×20×20 mm^3 in x×y×z sizes was cut from the distal epiphysis of a bovine femur, and the fluid components in the pore spaces were removed. Here, the x-, y-, and z-directions correspond to the longitudinal, transverse, and sagittal directions, respectively. The grayscale image of the trabecular structure was obtained by a 3D μCT system (SMX-160CTS, Shimadzu Corp., Kyoto, Japan) with a spatial resolution of 57 μm in three orthogonal directions. It was observed in the 3D μCT image that the trabecular orientation was strongest in the x-direction and weakest in the y-direction.

The cubic portions of 5.7×5.7×5.7 mm^3 were cut from the image at rotation angles of θ=0–90 deg on the axis of the z-direction perpendicular to the x-y plane, as shown in Fig. 1. The rotated x- and y-directions are designated as the x'- and y'-directions, respectively. From the cut images, numerical cancellous bone models with various trabecular-oriented angles of θ were constructed by downgrading the grayscale to binary using the threshold value between two peaks that repr-

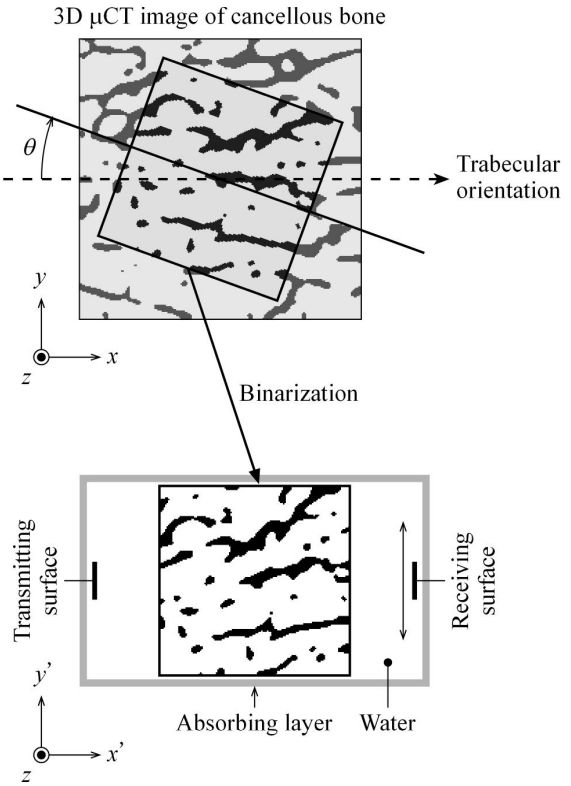

Figure 1. Schematic of simulation model for ultrasound propagation through cancellous bone with oblique trabecular orientation

esented the trabecular and pore components in a histogram of the image before cutting. It was assumed that all points corresponding to the pore space were perfectly filled with water. The porosities of the cancellous bone models, which were the percentages of the pore points in the models, were 0.83 (83%). To investigate the degree of the orientation at each trabecular-oriented angle θ, the ratio of the mean intercept length (MIL) in the x'-direction to that in the y'-direction was used, where MIL is defined as the averaged value of the intercept lengths that straight lines in an arbitrary direction generate in a medium region (i.e., trabecular or pore region) [23]. Figure 2 shows the degrees of the trabecular and pore orientations as a function of the oriented angle θ. Both orientations were strongest at the angle of θ=0 deg, and decreased with θ.

Simulation model

The region of the simulation model was 9.7×5.7×5.7 mm^3, in the middle of which the cancellous bone model was allocated, and the other was the water region. At the boundaries surrounding the whole region, Higdon's second-order absorbing boundary condition [24] was adopted. The transmitting and receiving surfaces, which were flat circles of 1.14 mm in diameter, were placed on the y'-z planes at x'=0 and 9.7 mm. The transmitting surface was fixed at the center on the plane, and the receiving surface was fixed at the center in the z-direction but moved from -2.28 to 2.28 mm at distances of 0.57 mm in the y'-direction. The value of y'=0 mm indicates the center position, and the positive and negative values of y' respectively indicate the upper and lower positions in Fig. 1. For the excitation condition, a pulsed particle displacement in the x'-direction of the ultrasound propagation was given at the corresponding points on the transmitting surface. The time function was a single sinusoid at 0.75 MHz multiplied by a Hamming window to set the center frequency at 1 MHz. The output was calculated as the summation of the pressures at all points on the receiving surface.

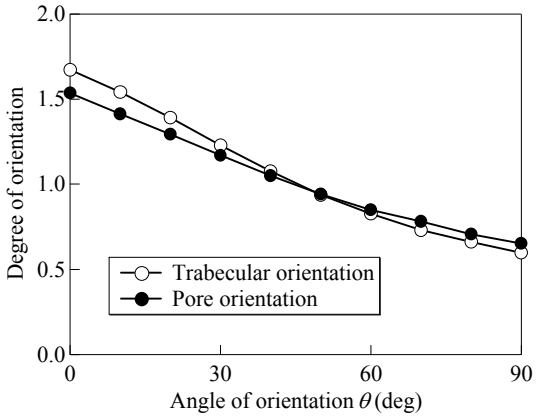

Figure 2. Degree of orientation for trabecular elements and pore spaces as a function of trabecular-oriented angle θ

Table 1. Physical parameter values of bovine cancellous bone model used in numerical simulations

	Trabecula	Water
First Lamé coefficient (GPa)	14.8	2.2
Second Lamé coefficient (GPa)	8.3	0
Density (kg/m^3)	1960	1000
Normal resistance coefficient (s^{-1})	8×10^4	75
Shear resistance coefficient (s^{-1})	8×10^5	0

The viscoelastic FDTD method (see [25] for detail) for simulating elastic wave propagation in a viscoelastic medium was used for the computation in the cancellous bone region, and the acoustic FDTD method for acoustic wave propagation was used in the water region. The spatial interval was 57 μm and the time interval was 4 ns. Table 1 lists the physical parameter values of bovine cancellous bone used in the FDTD simulations (see [25], in which the data of bone marrow is listed instead of the water data).

SIMULATION RESULTS

Observed waveforms

For each of the cancellous bone models with the trabecular-oriented angles of θ=0–90 deg, ultrasound pulse waveforms at various receiving positions y' were simulated. Figure 3 shows the change in the waveform received at the position of y'=0 mm with the oriented angle θ. At θ=0 deg, the fast and slow waves can be clearly observed. In general, the propagation speed of the fast wave is faster than the wave speed in the fluid (water) filling in the pore spaces, whereas the slow wave speed is almost the same with the speed in the pore fluid or slightly slower than it. Therefore, the fast and slow waves correspond to the waves propagating mainly in the trabecular elements and pore spaces, respectively [1]. It is practically considered that the fast wave can propagate in both trabecular elements and pore spaces, and that the slow wave can be also affected by the trabecular elements. In Fig. 3, the overlap of these waves becomes wider as the angle θ increases, and only a single wave can be observed above θ=40 deg because of the complete overlap. This change in the waveform is similar to the previously experimental results observed by declining the plate-like cancellous bone specimen [3] and by rotating the cylindrical specimen [5]. It is clear that in the case of the trabecular orientation parallel to the propagation direction, the fast and slow waves can travel mainly along the oriented trabecular elements and pore spaces, respectively [1], but that in the case of the perpendicular orientation, both waves travel mainly across the trabecular and pore orientations [3]. However, the wave propagation in the case of the oblique orientation is not sufficiently clarified.

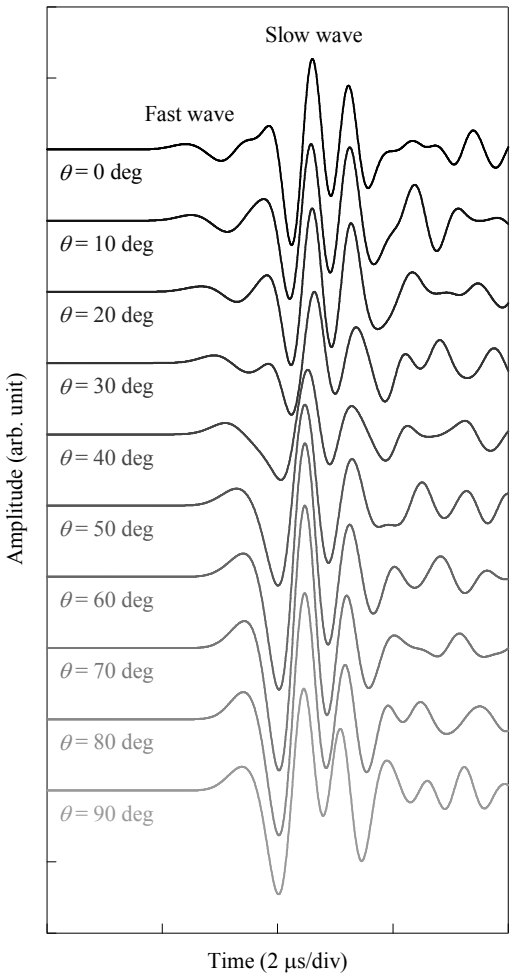

Figure 3. Simulated pulse waveforms propagating through cancellous bone with a porosity of 0.83 at various trabecular-oriented angles θ, which were received at center position of y'=0 mm

To investigate the effects of the oblique trabecular orientation on the propagation paths (or directions) of the fast and slow waves in cancellous bone, the wave amplitudes and propagation times were measured as a function of the receiving position y'. When the fast and slow waves were separated at low angles θ of trabecular orientation, the fast wave amplitude was measured from the first positive-peak amplitude of the corresponding fast waveform and the fast wave time was measured at the rise point. On the other hand, both the slow wave amplitude and time were measured using the second positive peak. The use of these measurement methods was the reason that the second peak of the fast wave and the first peak of the slow wave could interfere each other.

At high trabecular-oriented angles of θ, the single wave was observed. As shown in Fig. 1, the first peak of this wave arrived faster than the first peak of the slow wave observed at low angles of θ, whereas the second peak arrived at almost the same time with the slow wave. Considering the general speeds of the fast and slow waves in cancellous bone, the single wave can be regarded as the mixed fast and slow waves. The propagation properties of the mixed wave can be largely affected by the two waves. In fact, it has been shown using various experimental and theoretical models that the negative dispersion of the mixed wave speed could be explained by the overlap of the two waves [26, 27]. For the detailed understanding of the mixed wave properties, therefore, it is desirable to measure each of the fast and slow wave properties. In general, the separation of the fast and slow waveforms from the mixed waveform is very difficult, although several methods for separating the two waveforms in the case of the narrow overlap have been proposed [3, 18, 28, 29]. When the two waves were mixed, therefore, the fast and slow wave properties were extracted from the portions of the mixed waveform at which the respective properties strongly appeared.

In a previous study [6], it was shown from the similarity of the structural dependences that the mixed wave amplitude and speed, which were derived from the peak-to-peak amplitude and the propagation time at the rise point, corresponded to the slow wave amplitude and the fast wave speed, respectively. Then, the fast wave time was measured at the rise point of the mixed wave, and the slow wave amplitude was measured from only the second positive-peak amplitude in order to further reduce the effect of the two-wave overlap. The measurement of the slow wave time was also performed at the second positive-peak point. It was considered that the interference of the fast wave with the slow wave was slight because the slow wave amplitude was larger, as shown in Fig. 3. Moreover, it was assumed that the fast wave amplitude could be regarded as the first positive-peak amplitude. Although it was possibile that the first peak was affected by the slow wave, it was considered to strongly reflect the fast wave properties because the measured time at the first peak point showed the similar tendency to the time at the rise point which corresponded to the fast wave time.

Variations in fast and slow wave properties

Figure 4 shows the measured results for the wave amplitudes of the fast and slow waves at various trabecular-oriented angles θ, as a function of the receiving position y'. In Fig. 4, the wave amplitude at the angle of θ=0 deg and at the center position of y'=0 mm is set as 0 dB. In Fig. 4(a), the fast wave amplitude at θ=0 deg is maximum at y'=0 mm. The asymmetrical amplitude between the positive and negative positions of y' (upper and lower positions in Fig. 1) is considered to be due to the asymmetric trabecular structure. As the angle θ increases up to 20 deg, the position at which the fast wave amplitude is maximum becomes to shift upward. Above θ=20 deg, however, the fast wave amplitude increases with decreasing the position y', although the difference between the wave amplitudes at the upper and lower positions becomes smaller as the angle θ approaches to 90 deg. In addition, the fast wave amplitude generally increases with the angle θ. In Fig. 4(b), at the angles of θ=0 and 90 deg, the slow wave amplitude is almost symmetrical between the upper and lower positions. At the other angles, however, the slow wave amplitude at the lower position is larger than that at the upper position. In addition, the slow wave amplitude is generally large around θ=90 deg, although the variation with the angle θ is not so large.

Figure 5 shows the measured results for the propagation times of the fast and slow waves at various trabecular-oriented angles θ, as a function of the receiving position y'. In Fig. 5, the time differences from the simulated wave propagating only in water, which was received at the same position y', are shown, and therefore, the small and large time differences indicate the long and short propagation times, respectively. In Fig. 5(a), at the angle of θ=0 deg (and also 10 deg), the time differences of the fast wave at both upper and lower positions are smaller than that at the center position, which is considered to be because the trabecular elements in the cancellous bone model were oriented not perfectly parallel but radially. As shown in Fig. 1, the trabecular elements at the center position lay in the x-direction (x'-direction at θ=0 deg), but the elements at the upper and lower positions spread in the upward and downward directions, respectively. It is th-

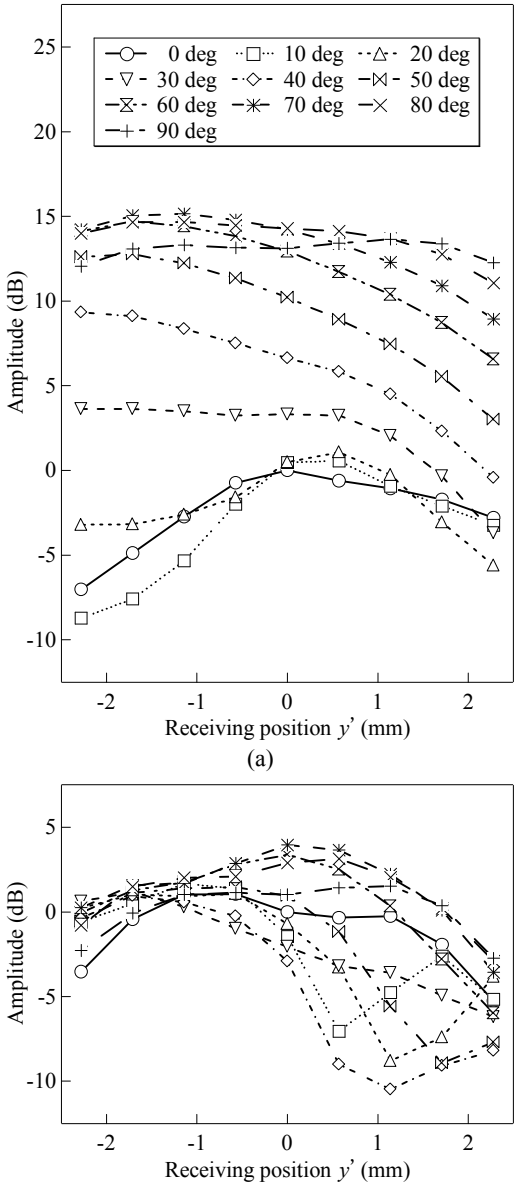

Figure 4. Wave amplitudes of (a) fast and (b) slow waves in cancellous bone with a porosity of 0.83 at various trabecular-oriented angles θ, as a function of receiving position y'

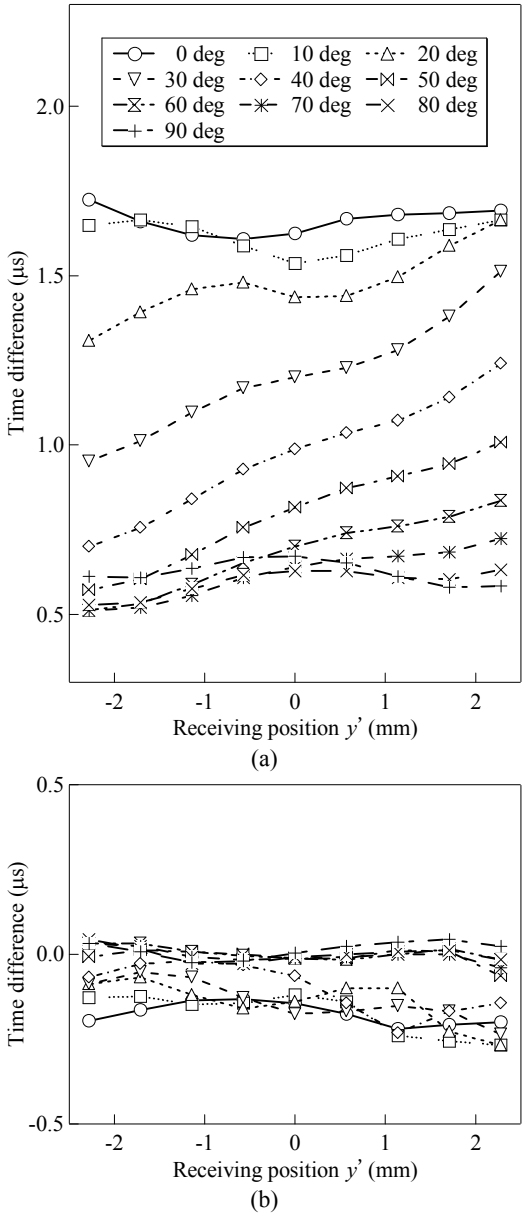

Figure 5. Propagation times of (a) fast and (b) slow waves in cancellous bone with a porosity of 0.83 at various trabecular-oriented angles θ, as a function of receiving position y'

erefore considered that the fast wave propagating along the trabecular elements was received not only at y'=0 mm but also at $y'\neq$0 mm. As the propagation distance at $y'\neq$0 mm was longer than that at y'=0 mm, the time difference became larger at $y'\neq$0 mm. On the other hand, the fast wave time at θ=20–80 deg decreases with the position y', although it scarcely varies near θ=90 deg. In Fig. 5(b), at the angles of θ=0–20 deg, the slow wave time, which is almost constant at every position of y', is longer than the propagation time only in water. As the angle θ increases up to 40 deg, the slow wave time only at the lower position becomes almost the same with the propagation time in water. At the higher angles, the slow wave time at every position becomes almost the same with the time in water.

DISCUSSION

The propagation paths (or directions) of the fast and slow waves at various angles θ of the trabecular orientation were investigated from the simulated results for the variations in the wave amplitudes with the receiving position y'. For the fast wave, the position of the maximum amplitude was slightly upper at the low trabecular-oriented angles below θ=20 deg but lower at the higher angles. As shown in Fig. 1, the direction from the transmitting to receiving surfaces at $\theta\neq$0 deg became closer to the trabecular-oriented direction (or x-direction) as the position y' shifted upward. Therefore, the larger wave amplitudes at the upper and lower positions of y' respectively mean that the wave propagations along and across the trabecular orientation are efficient. From the fact that the position of the maximum amplitude shifted upward, it is considered that at the low angles of θ, the propagation direction of the fast wave could change along the trabecular orientation. At the high angles, however, the fast wave amplitude became the maximum at the lower position, which means that the fast wave tended to turn to the opposite direction. On the other hand, at the oblique angles of θ, the slow wave amplitude at the lower position was larger than that at the upper position. This means that the slow wave tended to propagate across the trabecular orientation. At the oblique trabecular-orientated angles, both the fast and slow waves tended to propagate across the orientation. In a previous study [22] using stratified cancellous bone phantoms composed of periodically alternating the brass plates (as a substi-

tute for the trabecular plates) and water, however, the experimental results showed that the fast wave could propagate along the orientation of the trabecular plates, and that the slow wave only slightly transited from the propagation along the orientation to that across the orientation. These results are quite different from the simulated results in this study. This difference appears to be because the trabecular structure in the actual cancellous bone, unlike the ideal structure of the phantom, is not perfectly oriented. In addition, it appears to be the cause that the cancellous bone model used in this study had a high porosity of 0.83. When the porosity is high, the fast wave cannot efficiently propagate along the oblique trabecular orientation because the trabecular elements do not straightly connect in the oriented direction. In this case, the propagation of the slow wave across the oblique orientation can be generated because many pore spaces exist in the direction perpendicular to the orientation.

The propagation paths of the fast and slow waves were investigated from the variations in the propagation times with the receiving position y'. At the oblique trabecular-oriented angles θ, the fast wave time largely decreased with the receiving position y'. This means that the fast wave could propagate fastest along the trabecular orientation. For the fast wave, the relationship of the propagation speed to the angle θ is contrary to that of the wave amplitude, and therefore, the fastest wave is considered to be unable to propagate efficiently. On the other hand, the slow wave time at the lower angles of θ was slightly longer than the time at the higher angles, which means that the slow wave propagated slower along the orientation. This appears to be because the slow wave along the orientation propagates in the narrower spaces between the oriented trabecular elements. For the slow wave, contrary to the fast wave, the relationship of the propagation speed to the angle θ is the same with that of the wave amplitude, and the slowest wave is also considered to be unable to propagate efficiently.

In a previous study [6], it was shown that both the fast wave speed in the direction parallel to the trabecular orientation and the single wave speed in the perpendicular direction were much highly correlated with the MIL of the trabecular elements parallel to the wave propagation, and also that both the slow wave amplitude and the single wave amplitude were highly correlated with the MIL of the pore spaces perpendicular to the propagation. As described in the section "Observed waveforms", the single wave speed and amplitude in the previous study could be considered to correspond to the fast wave speed and the slow wave amplitude, respectively. For both parallel and perpendicular trabecular orientation, therefore, the high correlations were observed between the fast wave speed and the trabecular MIL and between the slow wave amplitude and the pore MIL. In this study, these correlations were investigated for oblique oriented directions. The trabecular MIL in the x'-direction and the pore MIL in the y'-direction were measured at the trabecular-oriented angle of θ=0-90 deg, and the correlation coefficients of the fast wave speed and the slow wave amplitude were calculated. Then, the fast wave speed and the slow wave amplitude at each receiving position y' were correlated to show the effects of the changes in the propagation paths (directions) of the fast and slow waves caused by the oblique trabecular orientation. The fast wave speed was derived from the fast wave time in Fig. 5(a) by assuming the straight propagation from the transmitting to receiving surfaces. The calculated correlation coefficients are shown in Fig. 6, as a function of the receiving position y'. Similarly to the results in the previous study, both correlation coefficients of the fast wave speed and the slow wave amplitude are high at the center position of y'=0 mm. It is therefore concluded that the high correlations of these wave properties can be satisfied for every direction of the trabecular orientation. In Fig. 6(a), however, the receiving position of the highest correlation is not center but slightly upper (y'=0.57 mm), despite of the correlation with the trabecular MIL in the x'-direction which is not the straight direction from the transmitting to receiving surfaces. Figure 6(b) also shows the highest correlation at y'=0.57 mm. These results appear to be due to the changes in the propagation paths caused by the oblique trabecular orientation.

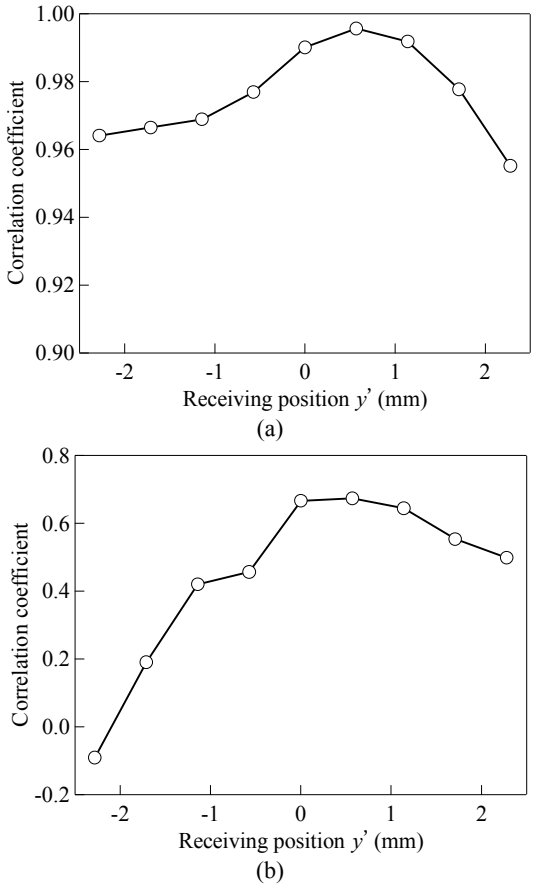

Figure 6. Correlation coefficients (a) between fast wave speed and mean intercept length (MIL) of trabecular elements in x'-direction and (b) between slow wave amplitude and MIL of pore spaces in y'-direction, as a function of receiving position y'

At high angles of the trabecular orientation, the fast and slow waves were mixed. In this case, it was possible that the wave properties measured from the mixed wave were affected by the other wave, although the measurements were performed at which the respective properties strongly appeared. In addition, it was possible that the simulated results in the section "SIMULATED RESULTS" were peculiar to the used cancellous bone model. To verify the generality and reproductivity of the results, then, the same simulations were performed using the distinct cancellous bone models constructed from eight positions of the bone specimen. The trabecular structures in these cancellous bone models were similar to the structure described in the section "Cancellous bone model", and the porosities were between 0.80 and 0.86. For both the fast and slow waves, the variations in the propagation properties with the trabecular-oriented angle were similar to those in "SIMULATED RESULTS", which indicates the verification of the generality and reproductivity. However, it is considered that the propagation paths of both waves largely depend on the trabecular structure, particularly the degree of the trabecular anisotropy. To investigate the dependence of the trabecular structure on the propagation paths, therefore, more simulations need to be performed using many cancellous bone models with various structures.

CONCLUSIONS

In this study, the propagation paths of the fast and slow waves in cancellous bone with oblique trabecular orientation were numerically investigated using FDTD simulations. From the simulated results for the variation in the wave amplitude of the fast wave with the receiving position, it was suggested that the fast wave could not efficiently propagate along the oblique trabecular orientation, except for at low angles of the orientation. The simulated results for the propagation time showed that the fast wave propagated fastest along the orientation. The slow wave also tended to propagate across the orientation, and in this case, both the wave amplitude and speed became large. Accordingly, both the fast and slow waves could efficiently propagate across the trabecular orientation, which causes the large overlap of these waves. It is therefore considered that the separation of the two waves is an uncommon phenomenon.

The simulated results were obtained for the cancellous bone models with strongly oriented trabecular structures and high porosities above 0.80, but it was considered that the propagation paths of both the fast and slow waves largely depended on the degree of the trabecular anisotropy. Therefore, further investigations using many cancellous bone models with various trabecular structures are required. Moreover, a future subject is that the relationships between the wave properties and the trabecular structure are clarified on the consideration of the changes in the propagation paths caused by the oblique trabecular orientation.

ACKNOWLEDGMENT

This study was supported by MEXT through a Grant-in-Aid for Young Scientists (B) (19700393). In addition, part of this study was supported by JSPS through a Grant-in-Aid for Scientific Research (B) (19360189), by the Academic Frontier Research Project on "New Frontier of Biomedical Engineering Research" of Doshisha University and MEXT, and by JSPS and CNRS under the Japan-France Research Cooperative Program.

The author would like to thank Mr. Ayumu Matsumoto at Akashi National College of Technology and Mr. Hiroki Soumiya at Doshisha University to assist in cutting the cancellous bone specimens and taking the 3D X-ray μCT images of the specimens.

REFERENCES

1 A. Hosokawa and T. Otani, "Ultrasonic wave propagation in bovine cancellous bone" *J. Acoust. Soc. Am.* **101**, 558-562 (1997)

2 A. Hosokawa, T. Otani, T. Suzaki, Y. Kubo, and S. Takai, "Influence of trabecular structure on ultrasonic wave propagation in bovine cancellous bone" *Jpn. J. Appl. Phys.* **36**, 3233-3237 (1997)

3 A. Hosokawa and T. Otani, "Acoustic anisotropy in bovine cancellous bone" *J. Acoust. Soc. Am.* **103**, 2718-2722 (1998)

4 G. Haïat, F. Padilla, F. Peyrin, and P. Laugier, "Fast wave ultrasonic propagation in trabecular bone: Numerical study of the influence of prosity and structural anisotropy" *J. Acoust. Soc. Am.* **123**, 1694-1705 (2008)

5 K. Mizuno, M. Matsukawa, T. Otani, M. Takada, I. Mano, and T. Tsujimoto, "Effects of structural anisotropy of cancellous bone on speed of ultrasonic fast waves in the bovine femur" *IEEE Trans. Ultrason. Ferroelectr. Freq. Control* **55**, 1480-1487 (2008)

6 A. Hosokawa, "Numerical analysis of variability in ultrasound propagation properties induced by trabecular microstructure in cancellous bone" *IEEE Trans. Ultrason. Ferroelectr. Freq. Control* **56**, 738-747 (2009)

7 C.M. Langton, S.B. Palmer, and R.W. Porter, "The measurement of broadband ultrasonic attenuation in cancellous bone" *Eng. Med.* **13**, 89-91 (1984)

8 P.J. Rossman, J.A. Zagzebski, C. Mesina, J. Sorenson, and R.B. Mazess, "Comparison of speed of sound and ultrasound attenuation in the os calcis to bone density of the radius, femur, and lumbar spine" *Clin. Phys. Physiol. Meas.* **10**, 353-360 (1989)

9 M.B. Tavakoli and J.A. Evans, "Dependence of the velocity and attenuation of ultrasound in bone on the mineral content" *Phys. Med. Biol.* **36**, 1529-1537 (1991)

10 J.A. Zagzebski, P.J. Rossman, C. Mesina, R.B. Mazess, and E.L. Madsen, "Ultrasound transmission measurements through the os calcis" *Calcif. Tissue Int.* **49**, 107-111 (1991)

11 P. Laugier, P. Giat, P.P. Droin, A. Saied, and G. Berger, "Ultrasound images of the os calcis: A new method of assessment of bone status" *Proc. 1993 IEEE Ultrason. Symp.*, 1993, pp. 989-992

12 R. Strelizki, A.J. Clarke, and J.A. Evans, "The measurement of the velocity of ultrasound in fixed trabecular bone using broadband pulses and single-frequency tone bursts" *Phys. Med. Biol.* **41**, 743-753 (1996)

13 T. Otani, "Quantitative estimation of bone density and bone quality using acoustic parameters of cancellous bone for fast and slow waves" *Jpn. J. Appl. Phys.* **44**, 4578-4582 (2005)

14 I. Mano, K. Horii, S. Takai, T. Suzaki, H. Nagaoka, and T. Otani, "Development of novel ultrasonic bone densitometry using acoustic parameters of cancellous bone for fast and slow waves" *Jpn. J. Appl. Phys.* **45**, 4700-4702 (2006)

15 I. Mano, T. Yamamoto, H. Hagino, R. Teshima, M. Takada, T. Tsujimoto, and T. Otani, "Ultrasonic transmission characteristics of *in vitro* human cancellous bone" *Jpn. J. Appl. Phys.* **46**, 4858-4861 (2007)

16 T. Otani, I. Mano, T. Tsujimoto, T. Yamamoto, R. Teshima, and H. Naka, "Estimation of *in vivo* cancellous bone elasticity" *Jpn. J. Appl. Phys.* **48**, 07GK05-1-07GK05-5 (2009)

17 P.H.F. Nicholson, R. Müller, G. Lowet, X.G. Cheng, T. Hildebrand, P. Rüegsegger, G. van der Perre, J. Dequeker, and S. Boonen, "Do quantitative ultrasound measurements reflect structure independently of density in human vertebral cancellous bone?" *Bone* **23**, 425-431 (1998)

18 L. Cardoso, F. Teboul, L. Sedel, C. Oddou, and A. Meunier, "*In vitro* acoustic waves propagation in human and bovine cancellous bone" *J. Bone Miner. Res.* **18**, 1803-1812 (2003)

19 E. Bossy, F. Padilla, F. Peyrin, and P. Laugier, "Three-dimensional simulation of ultrasound propagation through trabecular bone structures measured by synchrotron microtomography" *Phys. Med. Biol.* **50**, 5545-5556 (2005)

20 G. Haïat, F. Padilla, F. Peyrin, and P. Laugier, "Variation of ultrasonic parameters with microstructure and material properties of trabecular bone: A 3D model simulation" *J. Bone Miner. Res.* **22**, 665-674 (2007)

21 G. Haïat, F. Padilla, M. Svrcekova, Y. Chevalier, D. Pahr, F. Peyrin, P. Laugier, and P. Zysset, "Relationship between ultrasonic parameters and apparent trabecular bone elastic modulus: A numerical approach" *J. Biomech.* **42**, 2033-2039 (2009)

22 A. Hosokawa, "Effect of minor trabecular elements on fast and slow wave propagations through a stratified cancellous bone phantoms at oblique incidence" *Jpn. J. Appl. Phys.* **48**, 07GK07-1-07GK07-7 (2009)

23 W.J. Whitehouse, "The quantitative morphology of anisotropic trabecular bone" *J. Microsc.* **101**, 153-168 (1974)
24 R.L. Higdon, "Absorbing boundary conditions for difference approximations to the multi-dimensional wave equation" *Math. Comput.* **47**, 437-459 (1986)
25 A. Hosokawa, "Effect of trabecular irregularity on fast and slow wave propagation through cancellous bone" *Jpn. J. Appl. Phys.* **46**, 4862-4867 (2007)
26 K.R. Marutyan, M.R. Holland, and J.G. Miller, "Anomalous negative dispersion in bone can result from the interference of fast and slow waves" *J. Acoust. Soc. Am.* **120**, EL55-EL61 (2006)
27 C.C. Anderson, K.R. Marutyan, M.R. Holland, K.A. Wear, and J.G. Miller, "Interference between wave modes may contribute to the apparent negative dispersion observed in cancellous bone" *J. Acoust. Soc. Am.* **124**, 1781-1789 (2008)
28 M. Kaczmarek, J. Kubik, and M. Pakula, "Short ultrasonic waves in cancellous bone" *Ultrasonics* **40**, 95-100 (2002)
29 M.R. Marutyan, G.L. Bretthost, and J.G. Miller, "Bayesian estimation of the underlying bone properties from mixed fast and slow mode ultrasonic signals" *J. Acoust. Soc. Am.* **121**, EL8-EL15 (2007)